

Visual Investigation of Improvement in Extra-Heavy Oil Recovery by Borate-Assisted CO₂-Foam Injection

Seyed Amir Farzaneh¹ · Mehran Sohrabi¹

Received: 22 January 2016 / Accepted: 31 January 2018 / Published online: 13 February 2018
© The Author(s) 2018. This article is an open access publication

Abstract The significant reduction in heavy oil viscosity when mixed with CO₂ is well documented. However, for CO₂ injection to be an efficient method for improving heavy oil recovery, other mechanisms are required to improve the mobility ratio between the CO₂ front and the resident heavy oil. In situ generation of CO₂-foam can improve CO₂ injection performance by (a) increasing the effective viscosity of CO₂ in the reservoir and (b) increasing the contact area between the heavy oil and injected CO₂ and hence improving CO₂ dissolution rate. However, in situ generation of stable CO₂-foam capable of travelling from the injection well to the production well is hard to achieve. We have previously published the results of a series of foam stability experiments using alkali and in the presence of heavy crude oil (Farzaneh and Sohrabi 2015). The results showed that stability of CO₂-foam decreased by addition of NaOH, while it increased by addition of Na₂CO₃. However, the highest increase in CO₂-foam stability was achieved by adding borate to the surfactant solution. Borate is a mild alkaline with an excellent pH buffering ability. The previous study was performed in a foam column in the absence of a porous medium. In this paper, we present the results of a new series of experiments carried out in a high-pressure glass micromodel to visually investigate the performance of borate–surfactant CO₂-foam injection in an extra-heavy crude oil in a transparent porous medium. In the first part of the paper, the pore-scale interactions of CO₂-foam and extra-heavy oil and the mechanisms of oil displacement and hence oil recovery are presented through image analysis of micromodel images. The results show that very high oil recovery was achieved by co-injection of the borate–surfactant solution with CO₂, due to in-situ formation of stable foam. Dissolution of CO₂ in heavy oil resulted in significant reduction in its viscosity. CO₂-foam significantly increased the contact area between the oil and CO₂ significantly and thus the efficiency of the process. The synergy effect between the borate and surfactant resulted in (1) alteration of the wettability of the porous medium towards water wet and (2) significant reduction of the oil–water IFT. As a result, a bank of oil-in-water (O/W) emulsion was formed in the porous medium and moved ahead of the CO₂-foam front. The in-situ generated O/W emulsion has a much lower viscosity than the

✉ Seyed Amir Farzaneh
amir.farzaneh@hw.ac.uk

¹ Heriot-Watt University, Edinburgh, United Kingdom

original oil and plays a major role in the observed additional oil recovery in the range of performed experiments. Borate also made CO₂-foam more stable by changing the system to non-spreading oil and reducing coalescence of the foam bubbles. The results of these visual experiments suggest that borate can be a useful additive for improving heavy oil recovery in the range of the performed tests, by increasing CO₂-foam stability and producing O/W emulsions.

Keywords CO₂- foam · Heavy oil · Alkaline · Borate · Micromodel

1 Introduction

The total volume of heavy in-place oil resources, extra-heavy oils and tar sands identified on the planet has been estimated at 2200–3700 billion barrels (Huc 2011). The production of heavy and extra-heavy oils is on the rise, driven by ever increasing global energy consumption, rapid decline in the availability of light crude oils, and high oil prices. Thermal processes are usually applied to these reservoirs to enhance recovery by reducing the oil viscosity (Upreti and Lohi 2007). The majority of these thermal methods are a form of steam injection with cyclic steam stimulation (CSS) being one of the most successful of these techniques. Steam-assisted gravity drainage (SAGD) is a newer technique that has shown promise (Butler and McNab 1981; Butler and Stephens 1981). However, over half of heavy oil reservoirs are not suitable for thermal recovery processes (Farouq Ali 1997) for various technical and economic reasons. Thermal methods are also energy intensive, with a large carbon footprint and negative environmental impact due to their significant CO₂ production. There is, therefore, a need for developing non-thermal methods that can efficiently increase heavy oil recovery as an alternative to thermal methods.

Non-thermal methods mainly work by reducing the viscosity of heavy crude oils (by the addition of solvent), increasing the viscosity of the displacing fluids, or by reducing interfacial tension. A review of the major non-thermal methods of heavy oil recovery can be found elsewhere (Farouq Ali 1997; Farzaneh and Kharrat 2010 and Farzaneh and Dehghan 2012). Unfortunately, non-thermal methods have not been very successful in increasing heavy oil recovery. A survey of 62 field projects showed that only immiscible CO₂ injection has been marginally successful (Farouq Ali 1997).

A major technical challenge for immiscible CO₂ injection is the ability to control the mobility and sweep of the injected CO₂ correctly. This problem which stems from the adverse viscosity contrast between CO₂ and the reservoir fluids is more difficult in the case of extra-heavy crude oil. Generally, due to the *'unfavourable'* mobility ratio in CO₂ injection, flood profile control in gas floods is instrumental for a successful project (Klins 1984; Kulkarni 2003). Continuous research efforts are under way to improve the flood profile control in gas floods (McKean et al. 1999; Enick 2000). These include preparation of direct thickeners with gas-soluble chemicals which can increase the viscosity of gases by several orders of magnitude. Other methods have also been proposed, including modifications in the injected slug, such as the use of natural gas liquids (NGL) instead of water for highly viscous oils in low pressure, poorly producing and unconsolidated formations (Moritis 1995). Although these seem promising at the laboratory/simulator scale, important issues like feasibility, cost, applicability, safety and environmental impacts still need to be addressed (Moritis 1995). In addition, combining water and CO₂ injection under various injection strategies and modifications may offer efficient and viable solutions for improving oil recovery from

heavy oil reservoirs. In its simplest form, injecting CO₂, like a steam injection, reduces the viscosity of heavy oil. Viscosity reductions of up to two orders of magnitude can be achieved by CO₂ injection (Farzaneh et al. 2016). Water injected after CO₂ would then be able to drive the CO₂-diluted oil out of the reservoir and increase oil recovery. The performance of both waterflood and CO₂ injection can be further improved. For instance, heavy oils are known to be rich in natural surface active components. It is possible to utilize these natural surfactants in conjunction with other chemicals or additives to improve waterflood efficiency. The performance of CO₂ injection may also be enhanced by generating CO₂-foam in the reservoir. However, application of foam injection for improving heavy oil recovery has so far been very limited, and the effectiveness of the process and the impact of heavy oil on foam stability and flow are not known. Foam increases the effective viscosity of CO₂ and hence reduces its mobility. At the same time, it reduces the viscosity of heavy oil and increases its mobility.

Foam flood emerged in the 1960s as a promising technology for improving the reservoir sweep efficiency in steam and gas flood, due to its ability to reduce gas mobility (Schramm Laurier 1994). Successful field tests on foam application have also been reported (Shan and Rossen 2004). However, foam is a metastable system that coarsens spontaneously and decays due to liquid drainage from lamellae and plateau and capillary suction. An important parameter that should be considered regarding the ability of foam in mobility control is the effect of crude oil on foam stability. Oil becomes detrimental to foam at oil saturations above 5–20% (Schramm Laurier 1994). The success of foam injection for EOR depends on certain parameters, but the most important one is the ability of the surfactant to form a stable foam at reservoir conditions. Foam stability is the key parameter in foam flood design for mobility control purposes. Many factors affect the strength and stability of the foam in the reservoir, which have to be taken into account to select a suitable surfactant. For instance, while most of the surfactants can readily generate foam under standard conditions of low salinity water and in the absence of crude oil, very few can perform well in the presence of crude oil. A review of the details of important parameters which affect foam stability is given in our previous work (Farzaneh and Sohrabi 2013). The lowering of IFT using a surfactant for producing foam has been known for decades, and likewise the addition of alkali to surfactant (AS) is well known, due to decades of research in areas of chemical flood by many investigators (Nasr-El-Din and Taylor 1992; Reed and Healy 1977; Pope and Nelson 1978; Reisberg and Doscher 1956; Martin et al. 1985; Nelson et al. 1984; Lieu et al. 1982; Green and Willhite 1998). The addition of alkali can decrease IFT further, i.e. produce more stable foam (Guo et al. 2011). The alkali reacts with the naphthenic acids in the crude oil to generate soap, in-situ. The compositions of these naphthenic acids are given elsewhere (Shuler et al. 1989; Seifert 1975; Dunning et al. 1953; Pasquarelli and Wasan 1979). By combining the natural soap generated by alkali with a synthetic surfactant, a sharp decrease in IFT is obtained, or a lower amount of synthetic surfactant is required to achieve same (low) IFT level without alkali (Kovscek and Radke 1994; Rossen 1996; Zitha et al. 2006; Nguyen et al. 2007; Zitha and Du 2009). The use of alkali also reduces the adsorption of anionic surfactant on sandstones. Numerous laboratory studies (Hirasaki and Lawson 1985; Li et al. 2008) have demonstrated that foam could be used as a driver in an ASP process. However, the concern remains: is combining alkaline-surfactant (AS) with CO₂-foam, a viable process for heavier crude oils?

We have previously published the results of a series of foam stability experiments using alkali and in the presence of heavy crude oil (Farzaneh and Sohrabi 2015). The results showed that stability of CO₂-foam was decreased by adding NaOH, while it increased when adding Na₂CO₃. However, the highest increase in CO₂-foam stability was achieved by adding borate to the surfactant solution. Borate is a mild alkaline with an excellent pH buffering ability. Since

the previous study was performed in a foam column in the absence of a porous medium, in this paper, we present the results of a new series of experiments carried out in a high-pressure glass micromodel to visually investigate the performance of borate–surfactant CO₂-foam injection in an extra-heavy crude oil in a transparent porous medium.

The intention of this study is to further investigate the role of borate in enhancement of CO₂-foam behaviour as well as oil recovery improvement, to expand our understanding of extra-heavy oil/CO₂-foam performance and the impact of the addition of an alkaline on the stability of CO₂-foam. In this study, the pore-scale interactions of CO₂-foam and extra-heavy oil and the mechanisms of oil displacement and hence oil recovery performances are presented through image analysis of micromodel images. The synergy effect between borate and surfactants resulted in (1) alteration of the wettability of the porous medium towards water wet and (2) significant reduction of the oil–water IFT. As a result, a bank of oil-in-water (O/W) emulsion was formed in the porous medium and moved ahead of the CO₂-foam front.

2 Experimental

2.1 Micromodel Rig

A high-pressure micromodel setup was used to perform the visualization experiments described in this paper. Details of the micromodel rig can be found elsewhere (Sohrabi et al. 2000, 2001, 2004). A micromodel with a rock-look-alike porous pattern, which had been taken from a thin section photograph of a sandstone rock, was used in this study. Figure 1 shows a magnified section and the full-length picture of the micromodel. The pores and throats are shown in black and un-etched glass (grains) in white. The micromodel orientation was vertical with the inlet port at the top and the outlet at the bottom end of the model. The dimensions and properties of the micromodel are summarized in Table 1. To show the images of the micromodel at a suitable magnification, the image of a centre of the micromodel, which is typical of the micromodel, will be presented throughout this paper.

2.2 Fluids

A synthetic brine solution containing both NaCl and CaCl₂ salts was prepared and used in the coreflood tests. The brine solution had a total dissolved salt concentration of 10,000 ppm, consisting of 8000 ppm NaCl and 2000 ppm CaCl₂. The brine was de-oxygenated before injection into the storage cell. The heavy crude oil 'C' had API degree of 11.5 and viscosity of 8670 mPa.s at a test temperature of 50 °C. This crude oil has asphaltene content of 11.6%, an acid number of 3.38 mg KOH/g and a base number of 9.8 mg KOH/g. The (vapour) CO₂ has a purity of 99.8% and density and viscosity of 0.084 g cm⁻¹ and 0.017 mPa.s at 600 psig and 50 °C, respectively. The surfactant solutions used for the micromodel experiments were produced by mixing an appropriate volume of a surfactant into the brine solution.

The selection of surfactant and alkaline was based on an extensive set of fluid characterization tests, which are beyond the scope of this work and are reported in our previous study (Farzaneh and Sohrabi 2015). The surfactant solution which showed reasonable performance was then used for core flood experiments. Surfactant C1 (AOS 14+) was used in the micromodel tests involving surfactant injection. The active percentage and the critical micelle concentration of this surfactant are 39% and 0.3 vol%, respectively. The concentration of surfactant C1 used in this series experiments was 0.3 wt%. The alkaline solution used

Fig. 1 Pictures of the rock-look-alike micromodel. Pores and throats are shown in black and un-etched glass (grains) in white. A magnified section of the pore pattern **a** has been repeated a few times to make a half-length picture of the micromodel **b**

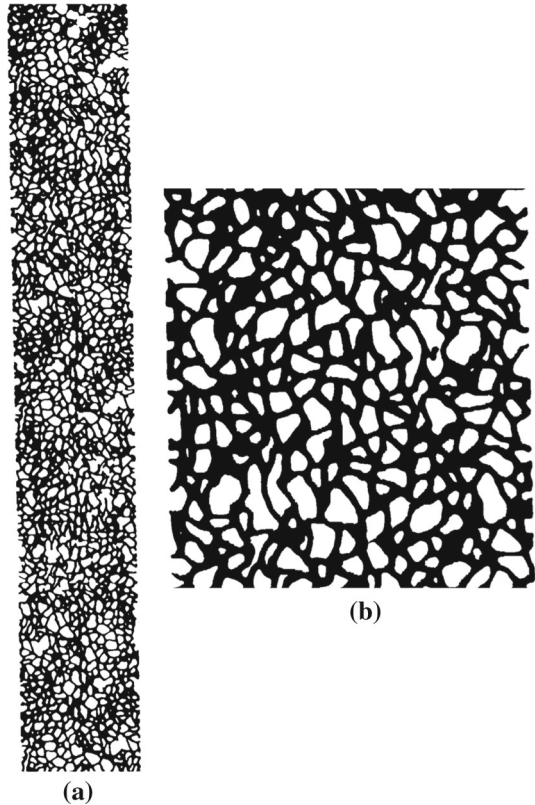


Table 1 Physical properties of the micromodel

Length (cm)	Width (cm)	Etch depth (μm)	Porosity	Permeability (D)
7	0.7	40	0.61	10

in these experiments was prepared by mixing 0.1 wt% borate in synthetic brine. Injection of fluids (oil, water, and CO_2) through the micromodel was performed at a slow rate of $0.005 \text{ cm}^3 \text{ h}^{-1}$, which corresponds to a frontal velocity of 2.27 ft day^{-1} . The same injection rate was used in all stages of the experiments, unless otherwise stated.

2.3 Experimental Procedure

Injection of oil, water, and CO_2 took place at a very slow rate of $0.005 \text{ cm}^3 \text{ h}^{-1}$, which corresponds to capillary numbers of $4.1\text{E-}7$ and $1.5\text{E-}7$ during waterflood and CO_2 injection, respectively. While oil injection was carried out from the bottom end of the micromodel, injection of water and CO_2 took place from the top end of the micromodel. The same experimental procedure was followed in all experiments, in which the micromodel was first saturated with water at the corresponding pressure and temperature of the experiment (600 psig at $50 \text{ }^\circ\text{C}$). To initiate the test, the crude oil was then injected from the bottom end of the micromodel and continued until no water saturation changes was observed in the micromodel. Then model

Table 2 List of presented micromodel experiments in this study

Exp. no.	Description	Pressure (psig)	Temperature (°C)	Sequences
1	Tertiary borate flood	600	50	1. Water flood 2. Borate flood
2	Tertiary borate–surfactant flood	600	50	1. Water flood 2. Borate–surfactant flood
3	Tertiary CO ₂ –foam flood	600	50	1. Water flood 2. Co-injection of CO ₂ /surfactant
4	Tertiary borate–CO ₂ –foam flood	600	50	1. Water flood 2. Co-injection of CO ₂ /borate–surfactant

was then flooded with water until oil production ceased. During foam injection, the rates were set to 0.001 and 0.004 (cm³ h⁻¹) for the surfactant or alkaline–surfactant solutions and the CO₂ phase, respectively.

All the micromodel tests were repeated at least once to examine repeatability of the results, and only repeatable tests were reported here. In Experiment 1, the waterflood period was followed by an extended period of tertiary borate flood. In Experiment 2, the period of waterflood continued with an injection of the tertiary borate–surfactant flood. In Experiment 3, the waterflood period was followed by an extended period of tertiary CO₂–foam flood. In Experiment 4, a similar procedure to that of Experiment 3 was followed. However, the co-injection of CO₂ and borate–surfactant started directly after the initial waterflood period. To ensure a constant and uniform CO₂/surfactant or CO₂/borate–surfactant ratio, the surfactant solution or borate–surfactant and the CO₂ were initially circulated through the bypass line for some time (up to 1 day) before going through the porous medium. During this period, the pressure of the injection and retract cells and the connecting lines were precisely monitored to ensure a state of fluid flow. The bypass line was then closed and the flow was diverted into the micromodel. The list of the micromodel experiments performed in this study is shown in Tables 1, 2.

3 Results and Discussion

3.1 Secondary Water Flood

Water flooding is the most common technique for secondary oil recovery in conventional oil reservoirs. It is also often employed in heavy oil reservoirs, because water injection is a relatively inexpensive and low-risk option and may be economical despite a low ultimate recovery due to adverse mobility ratio. However, its efficiency may be increased by various techniques, including by adding additives (alkaline, surfactant, polymer). This micromodel experiment was designed and performed to examine the process of secondary waterflood and its performance under the reservoir conditions of heavy crude oil ‘C’.

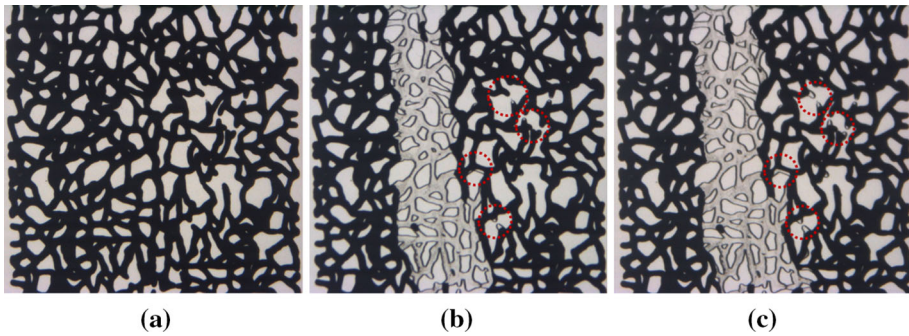


Fig. 2 Fluids distribution in a magnified section of the micromodel **a** after oil flood, **b** at the water BT ($t = 1.5$ h) and **c** at the extended period of waterflood ($t = 50$ h). The red dotted circles show where capillary force facilitated thickening of water layers and resulted in forcing the residual oil to leave the pores and the connected filaments of oil became continuously thinner (water saturation increases)

To begin the experiment, the micromodel was first saturated with synthetic brine. Next, crude oil 'C' was injected into the micromodel to establish the initial oil and water saturations. Oil injection continued until oil reached the other end of the micromodel. As expected, high oil saturation was achieved at the end of the oil flood period, due to the high oil/water viscosity ratio. Figures 2a and 3a show a magnified picture of the micromodel and the full-length picture of the micromodel after the oil injection period, in which the oil looks black and the connate water and glass grains look white.

After establishing initial oil and water saturations, the micromodel was flooded with water. Water was observed to channel through the oil phase, mainly flowing in the middle part of the porous medium, bypassing a large part of the oil. Figure 2b illustrates the same section of the micromodel at water breakthrough. Figure 3 shows a series of full-length images of the micromodel taken during water flood. Comparison of Fig. 3a through Fig. 3g reveals that, due to the high viscosity of the oil, water has opened a single finger through the porous medium and this channel has widened as the water injection continued. As the current micromodel is one-dimensional (much larger in length compared to its width), viscous instability demonstrates its effect via a single finger.

After water breakthrough, oil recovery continued, due to viscous forces, even as the injected water became the continuous phase in the micromodel. Comparison between Fig. 4a and d shows that, in heavy oil–water flood, the viscous force was more pronounced, even after water breakthrough. In contrast, capillary force becomes more prominent at an extended period of water flood. It is clearly revealed in Fig. 2c that, as water injection continued, the injected water supported the water layers on the pore walls, and these water layers became thicker. Subsequently, residual oil was forced to leave the pore and the connected filaments of oil became continuously thinner. In some pores, thickening of the water layers eventually resulted in rupture of these oil filaments, snap-off, or full recovery of the oil by piston type withdrawal. The dashed red circles in Fig. 2b, c show the areas of the micromodel which were affected by capillary force.

3.2 Tertiary Borate Flood

The recovery of heavy oil by water flooding is usually low, with a still significant amount of oil remaining at the end of water flood. Nevertheless, the waterflood efficiency may be increased by chemical additives. Alkaline flood is a process in which the pH of the flood

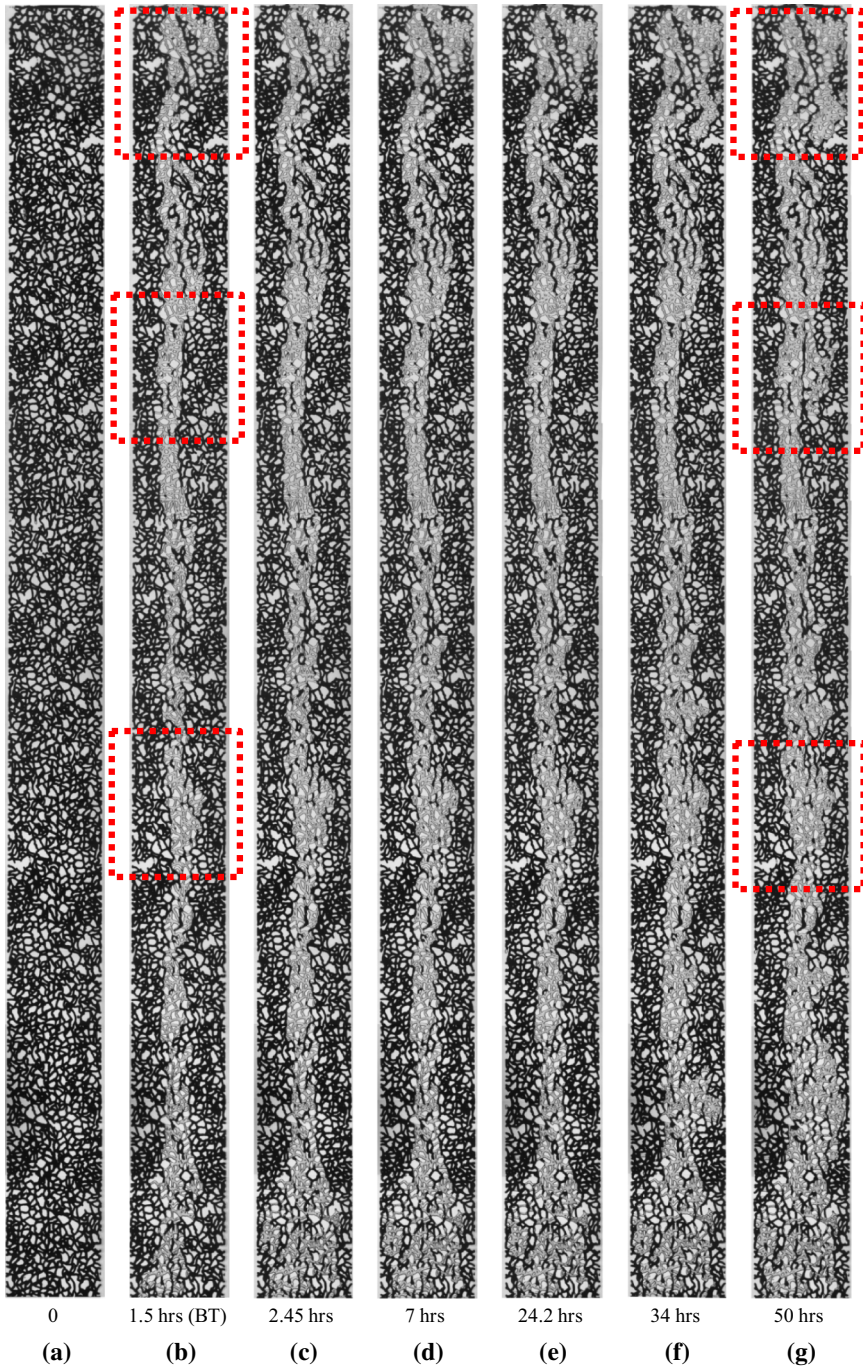


Fig. 3 Fluids distribution in the micromodel **a** after oil flood, **b** at water BT: due to the high viscosity of the oil, water has opened a single finger through the micromodel, **c** after 2.45 h, **d** after 7 h, **e** after 24 h, **f** after 34 h, **g** after 50 h of waterflood. The water channel has widened as the water injection continued, because of capillary force. The differences are shown in red rectangles

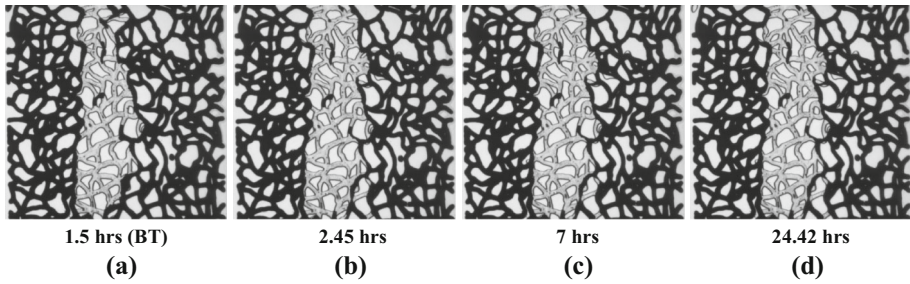


Fig. 4 Fluids distribution in a magnified section of the micromodel after **a** water BT, **b** 2.45 h, **c** 7 h, **d** 24.42 of water flood. The major changes occurred after water BT, due to viscous force, while the fluid pattern remained unchanged (capillary force, see Fig. 2)

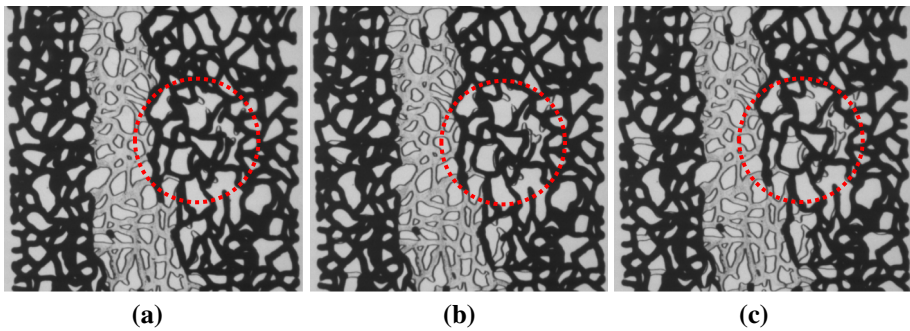


Fig. 5 Fluids distribution in the same magnified section of the micromodel **a** after 8 h of borate injection, **b** after 14 h of borate injection and **c** after 21 h of borate injection. The red dotted circle points out where capillary force facilitated thickening of water layers, resulting in forcing the residual oil to leave the pores, and the connected filaments of oil became continuously thinner, similarly to the behaviour observed during the waterflood test after breakthrough. However, this occurred faster than in the waterflood test

water is raised to a value of around 10–12 by adding different alkaline. The chemical reactions between alkaline materials and acidic species of the oil modify the interfacial properties of the crude oil/water/rock system and may result in additional oil recovery. The objective of this stage of Experiment 1 was to observe the effect of relatively low pH tertiary alkaline flood (pH was equal to 9.5 for borate with concentration of 0.1 wt%). The results of this micromodel test show that the injection of the borate solution increases the rate of oil recovery in the micromodel slightly compared to the plain water flood. Figure 5a–c shows the same magnified section of the micromodel after 8, 14 and 21 h of tertiary borate flood. Similarly to the behaviour observed during waterflood after breakthrough, the injected borate was found to flow in the form of film on the walls of the pores.

It is clear from Fig. 5a that the injected borate has initially displaced the residual water in the micromodel and has gradually spread via the water layer, especially towards the right-hand edges of the micromodel. Under the conditions of our experiments, the small incremental oil recovery by borate injection can be attributed to a wettability change towards more water-wet conditions and IFT reduction caused by the borate injection. The water layers were thicker in the images taken after 21 h of borate injection. Nevertheless, the reduction in interfacial tension, IFT, is not high enough using this alkaline to produce emulsion, and hence emulsification of the oil was not observed. The wettability alteration to more water wet could also be identified in the micromodel by the change of the shape of the oil/water

interface to a more non-spreading. Since the initial wettability condition of the micromodel was water wet, the change of wettability to more water wet, due to alkaline flood, did not result in additional oil recovery during the borate injection period.

It is worth mentioning that the tertiary surfactant flood was performed in our previous work (Emadi 2012), under the same conditions, to check the effectiveness of this surfactant in tertiary mode for improving recovery of this extra-heavy oil. After waterflood, the micromodel was flooded with the surfactant solution with the same concentration, which continued for a day. At this stage, some extra oil production was observed. As will be discussed later, this oil production is mainly due to a wettability change to more water-wet conditions and IFT reduction. This procedure was carried out so that when borate–surfactant was injected, the observed additional oil recovery could be attributed to borate–surfactant rather than the positive effects of surfactant injection.

3.3 Tertiary Borate–Surfactant Flood

The nature of “*bypassed*” oil in viscous oil reservoirs is significantly different from residual oil trapped by capillary forces in light oil reservoirs. To efficiently enhance the recovery of heavy oil, the injected fluids must be able to improve the viscosity ratio between the oil and injected water under the conditions of these experiments. The previous experiment (tertiary borate flood) was designed to show the impact of a limited amount of injected alkaline (borate) with a pH of 9.5 on oil recovery. A small incremental oil recovery by tertiary borate injection was observed, which was attributed to a wettability change towards more water-wet conditions and a reduction in interfacial tension (IFT). The relatively low volume of additional oil recovery is explained by an insufficient reduction in IFT due to the use of alkaline, coupled with insufficient oil emulsification to improve recovery. The results of Experiment 1 confirmed that the extra-heavy crude oil ‘C’ required a higher amount of alkaline to produce emulsions for improving mobility ratio. Experiment 2 was then designed to improve upon this result through the use of surfactant in addition to alkaline. The key objective of this experiment was to observe the effect of tertiary injection of a borate–surfactant (AS) flood.

After establishing initial oil and water saturations, as explained in the previous test, the micromodel was flooded with synthetic brine. The behaviour of waterflood was observed to be very similar to the previous micromodel experiment. Water was observed to channel through the central part of the porous medium, bypassing a large area of oil-filled pores. Figure 6a shows a section of the micromodel at the start of water flood, Fig. 6b shows the same part of the micromodel at water breakthrough, and Fig. 6c shows the same section after 48 h of secondary waterflood. Comparison of these figures reveals that the water has opened a single finger through the porous medium, which has widened as the water injection continued; this is a typical characteristic of heavy oil behaviour during waterflood. As the current micromodel is much larger in length compared to its width, viscous instability demonstrates its effect via a single finger. After the water breakthrough, oil recovery continued, due to viscous forces even as the injected water became the continuous phase in the micromodel. For this heavy oil waterflood, the viscous force was more pronounced, even after water breakthrough. In contrast, capillary force became more prominent after an extended period of waterflood. As water injection continued, the injected water supported the water layers on the pore walls, which then became thicker. Subsequently, residual oil was forced to leave the pore and the connected filaments of oil became continuously thinner. In some pores, thickening of the water layers eventually resulted in rupture of these oil filaments, snap-off, or full recovery of the oil by piston type withdrawal.

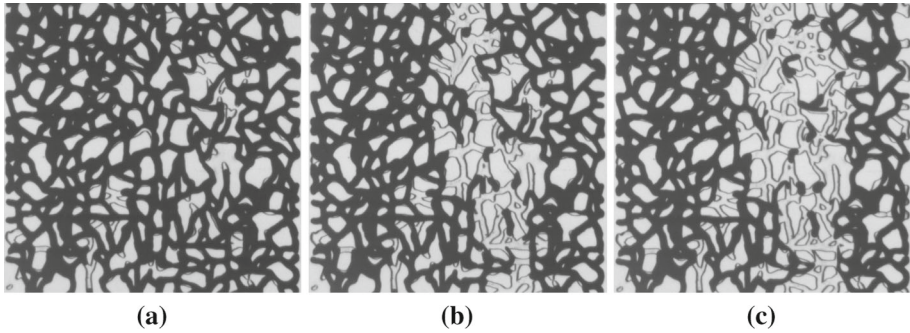


Fig. 6 Fluid distribution in a magnified section of the micromodel **a** after oil flood, **b** at the water breakthrough ($t = 1.5$ h) and **c** at the end of water flood ($t = 48$ h). Comparison of these figures reveals that water has opened a single finger through the porous medium, which has widened as the water injection continued

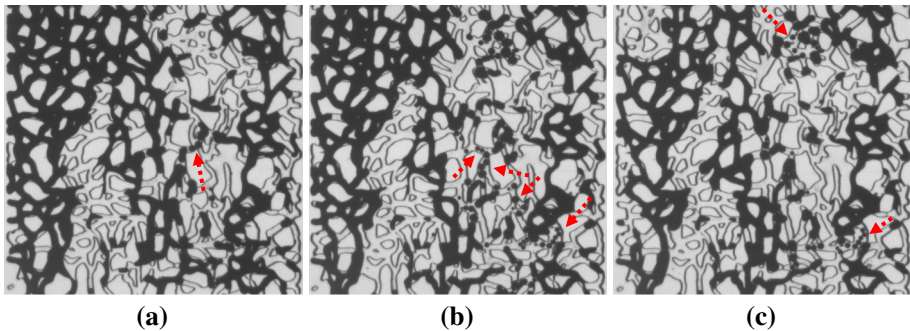
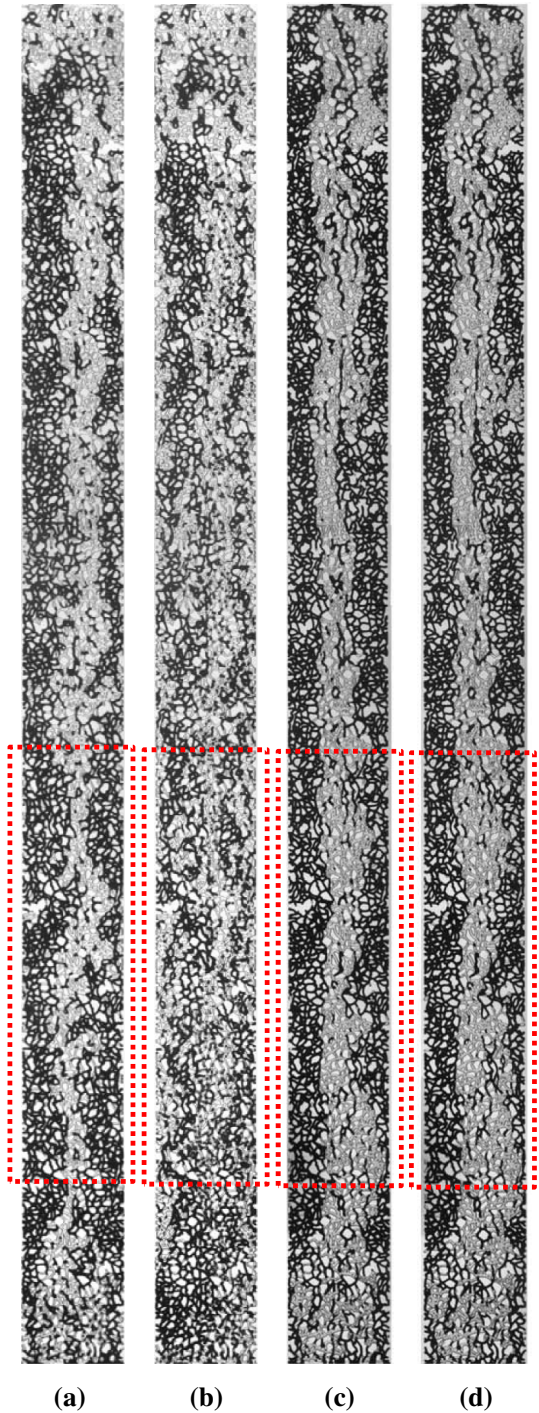


Fig. 7 Fluid distribution in a magnified section of the micromodel **a** after 4 h of AS flood, **b** after 8 h of AS flood and **c** after 24 h of AS flood. The strong emulsion forms in the middle of the micromodel due to the good synergy between borate and surfactant solution. It diverts flow towards the un-flooded area

To study the effect of AS flooding (low IFT and $\text{pH} = 9.5$) on enhanced extra-heavy oil recovery, a tertiary AS flood was carried out to compare the effectiveness of tertiary AS (0.1 wt% borate + 0.3 wt% C1) flood and tertiary alkaline (0.1 wt% borate) flood for extra-heavy crude oil 'C'. The results of this micromodel test show that the injection of the AS solution (0.1 wt% borate + 0.3 wt% C1) increased the rate of heavy oil recovery in the micromodel compared to tertiary alkaline flooding alone (0.1 wt% borate). Figure 7a–c illustrates the series of the same magnified section of the micromodel after 4, 8 and 24 h of AS flood.

Figure 8 shows a series of full-length images of micromodel taken during tertiary AS flood. It reveals that relatively high incremental oil recovery was obtained during tertiary AS flood (Fig. 8a, b) compared to the tertiary alkaline flood (Fig. 8c, d). This is due to the strong emulsification ability of AS solution (good synergy between alkaline and surfactant) as well as enhanced wettability modification to more water wet caused by the injected AS solution. The red arrows in Fig. 7 demonstrate the area in which O/W emulsion formed. Preliminary wettability measurements using the contact angle technique in a similar system with 0.3–0.5 wt% C1 surfactant have shown very strongly water-wet behaviour for un-aged quartz and mica samples (Sohrabi et al. 2004).

Fig. 8 Fluid distribution in the full-length images of micromodel **a** residual oil to waterflood in Experiment 2, **b** after 24 h of tertiary AS flood in Experiment 2, **c** residual oil to waterflood in Experiment 1 and **d** after 21 h of tertiary alkaline flood in Experiment 1. The red dotted rectangle shows that the sweep efficiency increased due to strong emulsification, in pictures **a** and **b**, and resulted in decreasing residual oil saturation, whereas the change in the residual oil saturation was negligible, as a result of the absence of synergy of borate and surfactant solution



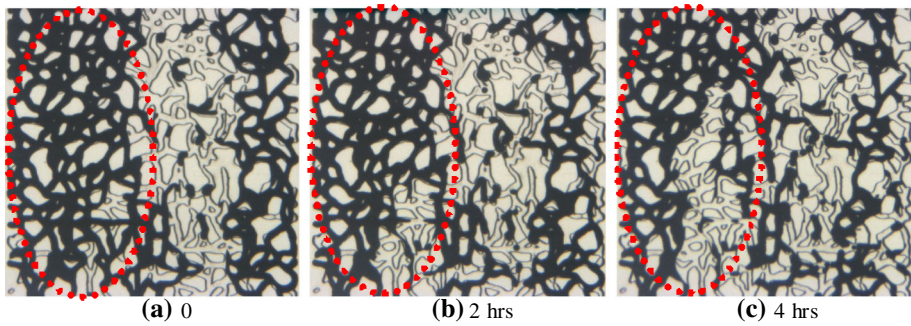


Fig. 9 Fluid distribution in the same magnified images of micromodel **a** residual oil to water flood, **b** 2 h, and **c** 6 h of tertiary AS flood. The flow direction was from top to bottom. The area within the red dashed oval illustrated the imbibition of aqueous phase into the waterflood residual oil from bottom to top, which was a good indication of wettability towards more water-wet condition

3.4 Discussion on Recovery Mechanisms During Borate–Surfactant Flood

To understand and describe the mechanisms involved in oil recovery by AS flood (Experiment 2), we use the observations made in the micromodel test. Based on the visualization results, two groups of mechanisms have been identified for oil recovery:

3.4.1 Wettability Modification

A change in wettability was observed towards more water wet, most likely through the formation of a surfactant bilayer at the glass/water/oil interface, or changes in double-layer forces. This would contribute towards additional oil recovery through water imbibition into the residual oil (Fig. 9). The initial wettability condition of the micromodel was weakly water wet to mixed wet; wettability could be enhanced to more water wet than in initial conditions due to the injected AS solution, although it is not directly attributed to the bulk of additional oil recovery.

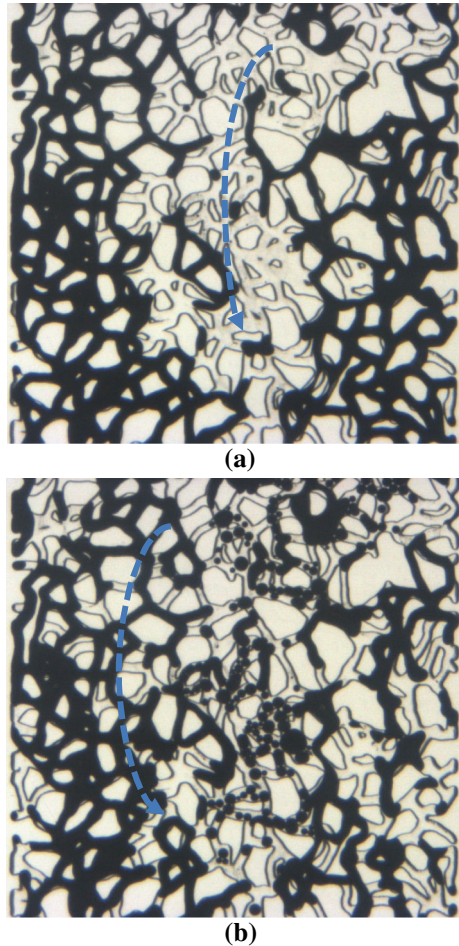
3.4.2 Emulsification

During the AS flood, the formation of an oil-in-water (O/W) emulsion is the dominant oil recovery mechanism in this process. Formation of these O/W emulsions is due to the effect of synergy between injected alkaline and surfactant. This O/W emulsion has a higher apparent viscosity than the injected AS solution and a lower viscosity than the oil phase. As a result of this mechanism, the water-flooded residual oil can be displaced more easily in the form of an emulsion, and at the same time, the higher viscosity of this emulsion causes better sweep and displacement efficiency. Figure 10 demonstrates the entrainment of O/W emulsion along with the aqueous phase and it then re-coalesces into the oil bank. Moreover, the non-uniform nature of the emulsions causes frequent blockage of the aqueous phase flow path. This modification causes the displacement and recovery of the residual oil in un-swept areas.

3.5 Tertiary CO₂-Foam Flood

The micromodel Experiment 3 was designed and performed to examine the performance of the process of CO₂-foam flood in the presence of extra-heavy crude ‘C’. The micromodel

Fig. 10 Fluid distribution in the same magnified images of micromodel **a** entrainment of O/W emulsion along with aqueous phase and **b** formation of a relatively thick oil bank resulted in recoalescence of the O/W emulsions. Moreover, the O/W emulsions caused frequent blockage of the flow path of the aqueous phase and resulted in flow path modification, which in line caused the recovery of the residual oil in un-swept areas. The blue arrows in the picture **a** and **b** show the water flow direction, which has been altered in the period of waterflood due to the emulsification and blockage of the first water flow path



results from Experiment 2 showed that AS injection could improve the recovery of extra-heavy crude oil 'C' to some extent. However, the higher viscosity of extra-heavy crude oil 'C' against produced O/W emulsions meant that there was an adverse mobility ratio. The main objective of this CO₂-foam flood experiment was to investigate if mobility control by CO₂-foam can effectively accelerate the process of oil displacement via decreasing the mobility ratio and the amount of CO₂ injection and consumption. The CO₂-foam flood test was carried out at same pressure and temperature as previous experiments.

After establishing initial oil and water saturations, as explained in previous tests, the micromodel was flooded with synthetic brine. The performance of waterflood was observed to be very similar to the previous micromodel experiments. Water was observed to channel through the central part of the porous medium, bypassing a large area of oil-filled pores. Figure 11a shows a section of micromodel at the start of waterflood, and Fig. 11b illustrates the same section of micromodel at the end of secondary waterflood (48 h).

Simultaneous injection of CO₂ and surfactant solution started after the secondary waterflood and continued for an extended period. Initially, the surfactant solution and CO₂ were simultaneously injected through the bypass line for a relatively long period, to ensure that

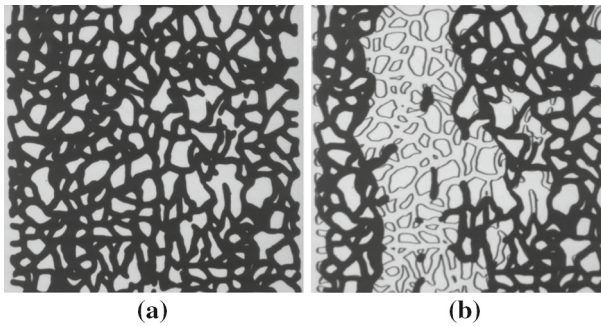


Fig. 11 Fluid distribution in a magnified section of the micromodel **a** after oil flood and **b** at the end of waterflood ($t = 48$ h) of Experiment 3

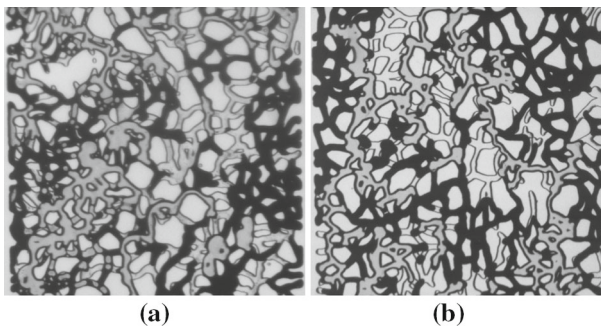


Fig. 12 Fluid distribution in the magnified section of the micromodel **a** after 10 min of CO₂-foam injection during Experiment 3 and **b** after an extended time of the tertiary CO₂ flood. The left picture confirms lower residual oil saturation as result of a higher number of moving interfaces between the injected CO₂ and the residual oil during injection of CO₂-foam

steady-state flow condition had been attained in the system. Then the flow of CO₂ and surfactant solution was diverted into the micromodel with a total injection rate of $0.005 \text{ cm}^3 \text{ h}^{-1}$ with a CO₂/surfactant solution ratio of 2 to 1. As the CO₂ and surfactant solution entered the micromodel, CO₂ bubbles (foam) were formed and the oil remaining after the preceding waterflood was displaced. Comparison of the results of CO₂/surfactant (foam) injection with the tertiary CO₂ flood results reported in our previous study (Farzaneh and Dehghan 2012) shows that much more oil was displaced by CO₂-foam, as the number of moving interfaces (contact areas) between injected CO₂ and the oil was significantly larger during CO₂-foam injection (Fig. 12).

During this process, CO₂-foam was destabilized by the surrounding oil. The spreading of oil over CO₂ bubbles causes weakening of the foam lamellae elasticity and consequently coalescence of the CO₂ bubbles as they flow through pores. The advancement of the CO₂-foam was observed to be associated with the formation of a thick bank of oil ahead, which itself helped oil recovery by reconnecting separated oil ganglia and displacing them towards the production point (Fig. 13a).

Another observation at this stage of the test was the formation of small water in oil emulsion (W/O) just ahead of the CO₂ front (Fig. 14). This W/O emulsion can increase the resistance to the flow of CO₂-foam through the micromodel and improve displacement efficiency of the process. Figure 14 shows the same magnified section of the micromodel at an early stage of

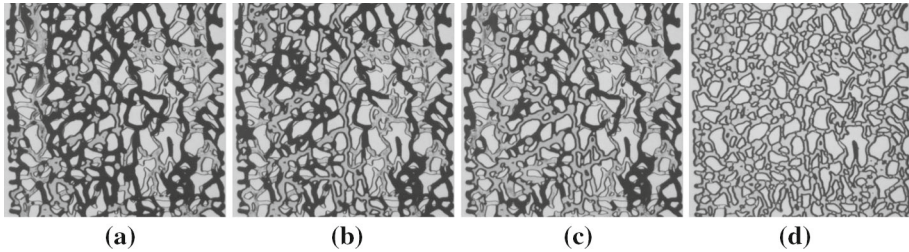
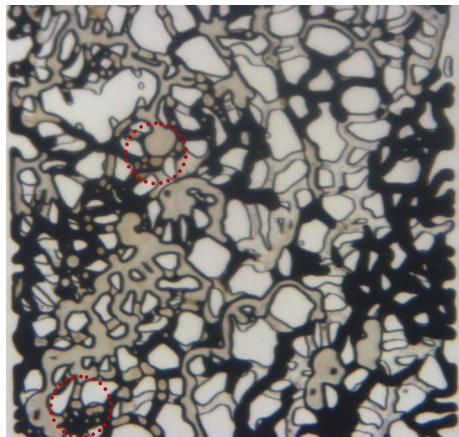


Fig. 13 Fluid distribution in the same magnified section of the micromodel **a** after 1 h of the CO₂-foam injection. The CO₂-foam was destabilized by the surrounding oil as the spreading of oil over CO₂ bubbles causes weakening of the foam and coalescence of the foam bubbles as they flow through pores, **b** after 2 h of CO₂-foam injection. The resistance to flow of the foam increased and, therefore, it was diverted to un-swept areas of left-hand side of the micromodel that still held significant residual crude oil, **c** after 4 h of the CO₂-foam injection as the oil residual oil saturation decreased further, the CO₂-foam became increasingly more stable and stronger and increasingly targeted the oil remaining in hard-to-reach areas of the micromodel (left-hand side), and **d** after 50 h of the CO₂-foam injection. The advancement of the CO₂-foam was observed to be associated with the formation of a thick bank of oil ahead, which itself helped oil recovery by reconnecting separated oil ganglia and displacing them towards the end of the micromodel

Fig. 14 Generation of water in oil emulsion during advancement of CO₂-foam in a magnified section of the micromodel. The red circle shows the flowing of CO₂-foam and water droplets. The mechanism was a flow in the form of emulsion or a small fragment of oil in between CO₂ bubbles and also film flow over the pore walls



CO₂-foam injection (foam BT). The displacement mechanism was observed to change from direct displacement to flow, in the form of an emulsion or a small fragment of oil in between CO₂ bubbles, and also film flow over the pore walls.

As more oil was displaced, and less oil remained in the path of the flowing foam, the foam became more stable and stronger (smaller CO₂ bubbles) and hence, the resistance to flow of the foam increased and, therefore, it was diverted to un-swept areas of the porous medium that still held significant crude oil (Fig. 13b). As the oil saturation decreased further, the CO₂-foam became increasingly more stable and stronger and increasingly targeted the oil remaining in hard-to-reach areas of the porous medium (Fig. 13c). After 50 h of CO₂-foam flood more than 90% of the oil remaining after waterflood was displaced and recovered and the remaining oil was located mostly in dead-end pores (Fig. 13d).

Fig. 15 Fluid distribution in the magnified section of the micromodel at the end of waterflood period (48 h)



3.6 Tertiary Alkaline–CO₂-Foam Flood

The micromodel results from Experiment 2 showed that the injection of borate–surfactant could improve recovery of extra-heavy crude oil ‘C’ to some extent, compared to water flood. Otherwise, the micromodel results from Experiment 3 proved that the extra-heavy crude oil ‘C’ was very effectively displaced by a series of mechanisms, as mentioned, taking place during CO₂-foam injection, if CO₂-foam was injected for an extended period. We also highlighted the pore-scale mechanisms by which CO₂-foam increased oil recovery and showed that very high oil recovery could be achieved by CO₂-foam injection through some active mechanisms. However, foams tend to become unstable when they come in contact with crude oil; therefore, for EOR applications, it is vital that the foam remains stable under reservoir conditions in contact with crude oil.

The main objective of this alkaline–CO₂-foam (AS–CO₂-foam) injection test was to investigate the impact of borate, which is a mild alkaline with high salinity tolerance, on CO₂-foam stability. The objective was to co-optimize the improvement of mobility control by CO₂-foam (by improvement in foam stability) with an improvement in oil emulsification (synergy effects between alkaline and surfactant).

The oil flood was quite similar to the oil flood of the previous experiments, regarding mechanisms of displacement and resultant water and oil saturations. Waterflood started after establishing the initial oil and water saturations in the micromodel and continued for 48 h. Figure 15 illustrates the magnified section of the micromodel at the end of the waterflood period, and Fig. 17a, b illustrates the corresponding full-length picture of the micromodel at the start and end of waterflood, respectively. After this period of water flooding, CO₂ and the alkaline–surfactant solution with a concentration of 0.1 wt% borate and 0.3 wt% C1 were co-injected simultaneously through the micromodel.

After water flooding, and before the simultaneous injection of CO₂ and alkaline–surfactant solution began, the micromodel was flooded with the alkaline–surfactant solution for 10 h. This was carried out so that any additional oil recovery due to alkaline–surfactant (AS) itself could be identified and later, when the co-injection of CO₂ and alkaline–surfactant began the additional oil recovery could be attributed to CO₂-foam rather than the effects of the alkaline–surfactant injection. At this stage (alkaline–surfactant injection), some additional oil recovery was observed. This oil production is attributed to wettability change to more

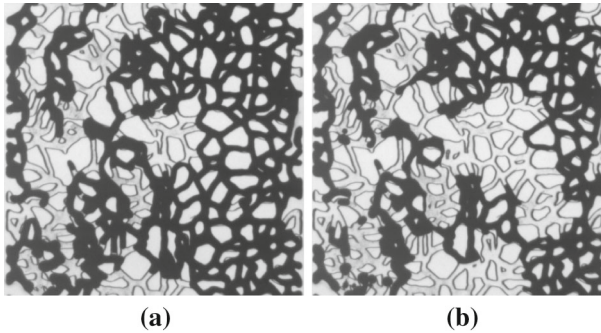


Fig. 16 Fluid distribution in a magnified section of the micromodel **a** at the start of the tertiary alkaline–surfactant flood **b** at the end of the tertiary alkaline–surfactant flood (Experiment 4). This oil production is attributed to wettability change to more water-wet conditions and IFT reduction caused by the surfactant as well as the flow of O/W emulsion caused by the alkaline

water-wet conditions and IFT reduction caused by the surfactant as well as the flow of O/W emulsion caused by the alkaline, which is referred to as “synergy effect” of alkaline and surfactant solution. Figure 16a illustrates the magnified section of the micromodel at the start of AS flood. Comparison of this picture with Fig. 16b, which was captured at the end of the AS flood period, shows some oil production and redistribution during the alkaline–surfactant solution injection period.

Figure 17c illustrates the corresponding full-length picture of the micromodel at the end of the tertiary borate–surfactant flood period. It can be clearly observed in the pictures that the injection of the AS solution increased the rate of extra-heavy oil recovery in the micromodel compared to plain waterflood. The injected AS initially displaced the remaining oil from the central part of the micromodel and then moved it towards the right and left edges of the micromodel progressively.

Our observation shows that, in the micromodel, the oil recovery increment by AS injection could be related to two categories of mechanisms, based on the timing of their appearance. The first type of mechanism in which caused oil remobilization and reconnection of the trapped oil consists of the wettability change (to strongly water wet) and interfacial tension (IFT) reduction. Shortly, after the arrival of the AS solution in the micromodel the redistribution of the trapped crude oil due to these two mechanisms was observed. The reduction of water–oil IFT could be observed visually by displacing of the joined oil ganglia and of the trapped oil droplets in small pore bodies. The wettability alteration to more water-wet conditions as described before. As these two mentioned oil recovery mechanisms occur in the micromodel virtually at the same time, it is difficult to identify their separate contribution to the observed additional oil recovery during the AS injection period. The combination of these two mechanisms enhances oil recovery by reducing the adhesion forces between oil and the porous medium and by reducing capillary forces. This initiates the formation of a bank of oil in front of the injected AS solution. Emulsification of the heavy crude oil in water was also observed (Fig. 18). This mechanism is closely linked to and is a result of the previous two mechanisms (wettability change and IFT reduction), but since it is a distinct oil displacement mechanism by itself and seems to occur at later times during AS injection, it should be considered separately. From the visualization results, it appears that, when a certain lower limit of IFT between water and oil is reached, and under strongly water-wet conditions, trapped oil ganglia start to move, forming small droplets of oil in the AS solution.

Fig. 17 Fluid distribution in a magnified section of the micromodel **a** just before starting waterflood **b** at the end of water flood, 48 h and **c** at the end of the tertiary borate–surfactant flood (Experiment 4). It shows that the injection of the AS solution increased the oil production in the micromodel compared to plain waterflood. The injected AS initially displaced the remaining oil from the water invaded area of the micromodel and then gradually spread towards the right and left edges of the model because of emulsification and flow diversion

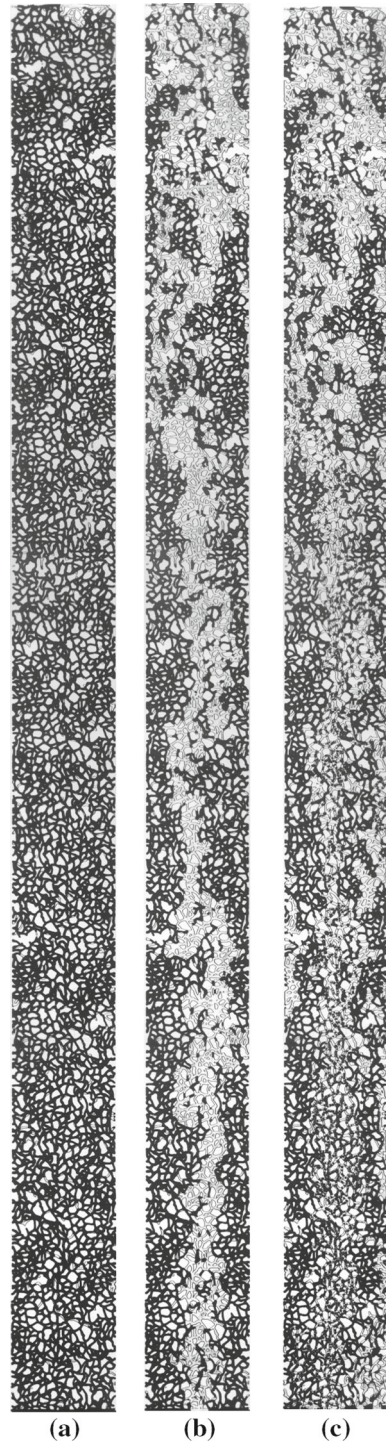
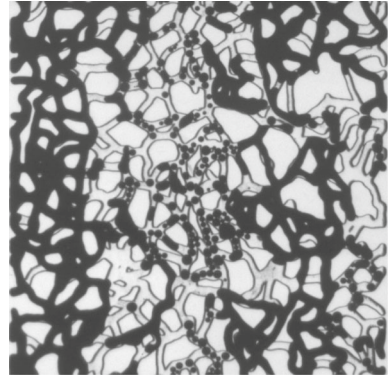


Fig. 18 Fluid distribution in the magnified section of the micromodel during the period of the AS flood. Strong emulsification was produced, due to the synergy between alkaline and surfactant solutions



At later times, as the IFT between oil and the aqueous phase drops to lower values (possibly due to the reaction between acidic components of the oil and alkaline material in the aqueous phase) the size of these oil droplets becomes smaller as well (Fig. 19).

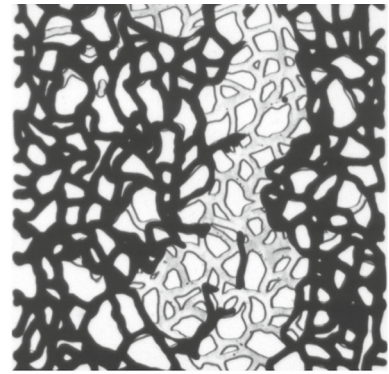
The contribution of these two mechanisms to additional oil recovery is different in light and heavy oils. In the light oil, where most of the oil is trapped due to capillary forces and the acidic species in the oil phase are not enough to generate ultra-low IFT, IFT drop, and wettability alteration towards more water-wet conditions are responsible for most of the additional recovery. However, as the crude oil becomes heavier and reaches in the surface active materials, the emulsification plays a more important role in the oil recovery process. In this part of the test, most of the incremental oil recovery was obtained through the emulsification mechanism. Figure 20a shows a magnified section of the micromodel that has not been passed by a front of produced O/W emulsions, while Fig. 20b shows the same section at the AS front, where emulsification is taking place.

After the period of AS injection, simultaneous injection of AS solution and CO₂ started and continued for an extended period. Initially, the AS solution and the CO₂ were simultaneously circulated through the bypass line for a relatively long period to ensure that steady-state flow has been attained. Then the flow of AS solution and CO₂ was diverted into the micromodel with a total rate of 0.005 cm³ h⁻¹, with a CO₂/AS solution injection ratio of 2:1.

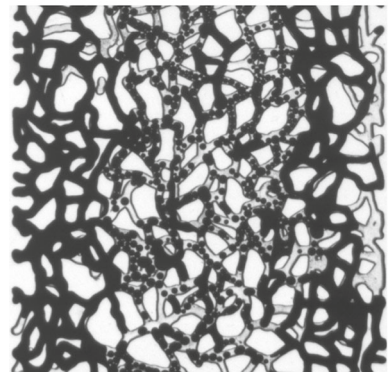
Compared to the previous foam experiment, much stronger foam formed at the top of the micromodel where AS and CO₂ were co-injected. Since every other parameter of the test was the same as the previous foam injection experiment, the observed increase in the strength and stability of the foam in this experiment is attributed to the borate (alkaline) that had been added to the surfactant solution. Figure 20a shows a magnified image of a section of the micromodel after 5 min of the beginning of AS–CO₂-foam injection.

An important observation at the start of the injection of AS–CO₂ was the formation of oil-in-water (O/W) emulsion just ahead of the CO₂-foam front. The O/W emulsion formed as a result of the mixing of AS–CO₂-foam and residual oil in the porous medium. These O/W emulsions improve the displacement efficiency of the oil by reducing the effective viscosity of the oil and by increasing the resistance to the flow of AS–CO₂-foam through the micromodel (Fig. 21). The O/W emulsion banked up oil, which moved ahead of the AS–CO₂-foam. This thick bank of oil itself caused reconnection of the separated oil ganglia and moved the oil towards the production end of the porous medium. The formation of the oil bank can be seen from the increase in the saturation of the oil in Fig. 20b compared to the oil saturation at the start of the AS–CO₂ injection in this same section of the micromodel which is shown in Fig. 20a. After 25 h of AS–CO₂-foam flood more than 92% of the oil remaining

Fig. 19 Fluid distribution in the magnified section of the micromodel during the period of the tertiary AS flood. **a** The path of water at the end of waterflood, **b** a bank of oil was formed in front of the AS front as a result of the emulsification process



(a)



(b)



(a)

(b)

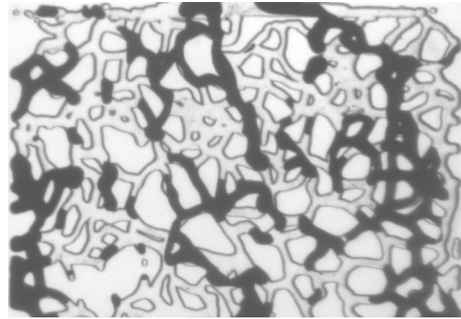
(c)

Fig. 20 Fluid distribution in a magnified section of the micromodel **a** after 5 min. of AS–CO₂-foam flood, **b** after 10 min of AS–CO₂-foam flood. The O/W emulsions formed an oil bank, due to its lower viscosity than extra-heavy crude oil 'C' itself and (c) after 25 h of the alkaline–CO₂-foam injection

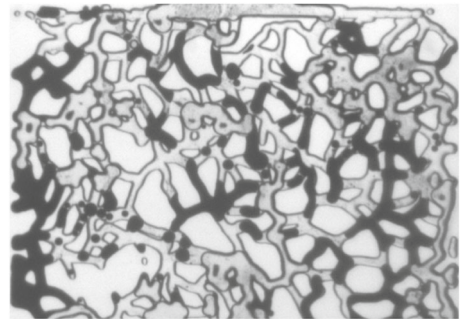
after waterflood was displaced and recovered and the remaining oil was located mostly in dead-end pores (Fig. 20c).

After just 10 min of simultaneous AS/CO₂ injection, a stable CO₂-foam occupied the top (injection point) of the micromodel, and as the foam strength increased and the resistance to its flow increased, foam was diverted to un-swept areas of the porous medium, which still

Fig. 21 Fluid distribution in the magnified section of the micromodel after 5 min of AS–CO₂–foam injection. The O/W emulsions formed as a result of the mixing of AS–CO₂–foam and residual oil in the micromodel



(a) Before AS–CO₂–Foam



(b) 5 min after AS–CO₂–Foam

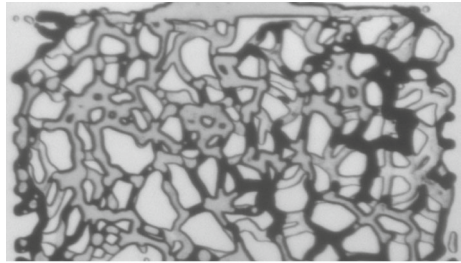
had a significant amount of oil and O/W emulsion. Compared to the previous CO₂–foam injection test, in the AS/CO₂ injection test, the pattern of flow was different and the oil had less spreading tendency and, as a result, the foam was stronger and more stable. Figure 22 compares the performance of CO₂–foam in Experiment 3 (CO₂–foam injection), in which no alkaline had been used, with the performance of the AS–CO₂–foam. Higher numbers of CO₂ bubbles could be seen in the AS–CO₂–foam test. Additionally, as can be seen from Fig. 22a, the oil has a lower tendency towards the surface of the porous medium, as the surface was more water wet in the AS–CO₂ test. This can be seen by the lack of grey surfaces, which are clearly visible in Fig. 22a, b. The grey areas in Fig. 22b are caused by the oil smearing on the surface of the porous medium.

3.7 Discussion on Recovery Mechanisms During Borate-CO₂-Foam Flood

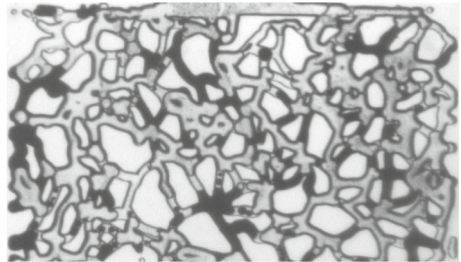
The brown, red, and green arrows in Fig. 23 show the approximate location of the “residual oil”, “O/W emulsion” and “CO₂–foam” banks, respectively. It should be noted that the arrows only show the approximate location of boundaries, as the change from one phase to another is very gradual. It means that the CO₂–foam phase and the O/W emulsion phase exist throughout the micromodel. In the CO₂–foam region, oil droplets can be seen and similarly in the O/W emulsion bank, the CO₂ phase can be seen, but in a lower amount and with fewer bubbles.

Figure 23a–c illustrates the full-length images of the micromodel during AS–CO₂–foam injection, at the start of the test and at 10 and 60 min after the start of the test, respectively. The figures show the formation of the bank of oil emulsions ahead of the foam front. At this stage, as the foam front went further, the bank of O/W emulsion grew and displaced the residual oil within the micromodel (O/W emulsion has much lower viscosity compared to

Fig. 22 Foam distribution in the magnified section of the top of micromodel after 10 min of **a** CO₂-foam injection, **b** AS-CO₂-foam injection. Stronger and more stable foam was obtained during the AS-CO₂-foam experiment due to the addition of alkaline (borate)



(a) Top of micromodel after 10 minutes of CO₂-foam injection



(b) Top of micromodel after 10 minutes of AS-CO₂-foam injection

residual oil). A double displacement mechanism was observed in which foam displaced the oil emulsion and oil emulsion displaced oil. Figure 23b–d shows that the formation of the oil emulsion bank happened faster than the formation of the bank of foam.

Figure 23d, e illustrates the full length of the micromodel during the AS-CO₂-foam injection test at 4 and 15 h after the start of injection. As more oil was produced and the saturation of the oil decreased, the foam bank developed faster and further displaced the oil emulsion bank towards the production end of the micromodel. After 25 h of AS-CO₂-foam flood, more than 90% of the waterflood residual oil was displaced and recovered (Fig. 23f). As the oil saturation decreased to below 10%, the AS-CO₂-foam became very stable, and the foam washed out the remaining oil, which was located mostly in the hard-to-reach and dead-end pores (Fig. 23f). At this stage of the test the displacement mechanisms were direct displacement of the bank of oil emulsion via foam, and the flow of small fragments of oil in between the foam bubbles, and also oil film flow over the pore walls. On the other hand, the stability of the foam was higher than that of the foam produced in Experiment 3, which was attributed to the presence of borate.

3.8 Compatibility of CO₂ and Borate

The question here is that since the dissolution of CO₂ in water results in the formation of carbonic acid and a subsequent reduction in pH, co-injection of CO₂ and borate may lead to neutralization of the effect of borate (alkaline). While this would be a concern in the injection of traditional alkaline (e.g. NaOH), it was not observed in our experiments, where borate was used. The explanation is that borate is a mild alkaline with strong buffering effect. Therefore, its positive effects, which mainly stem from lowering interfacial tension (IFT), are still present, even when co-injected with CO₂. However, this was not observed in the

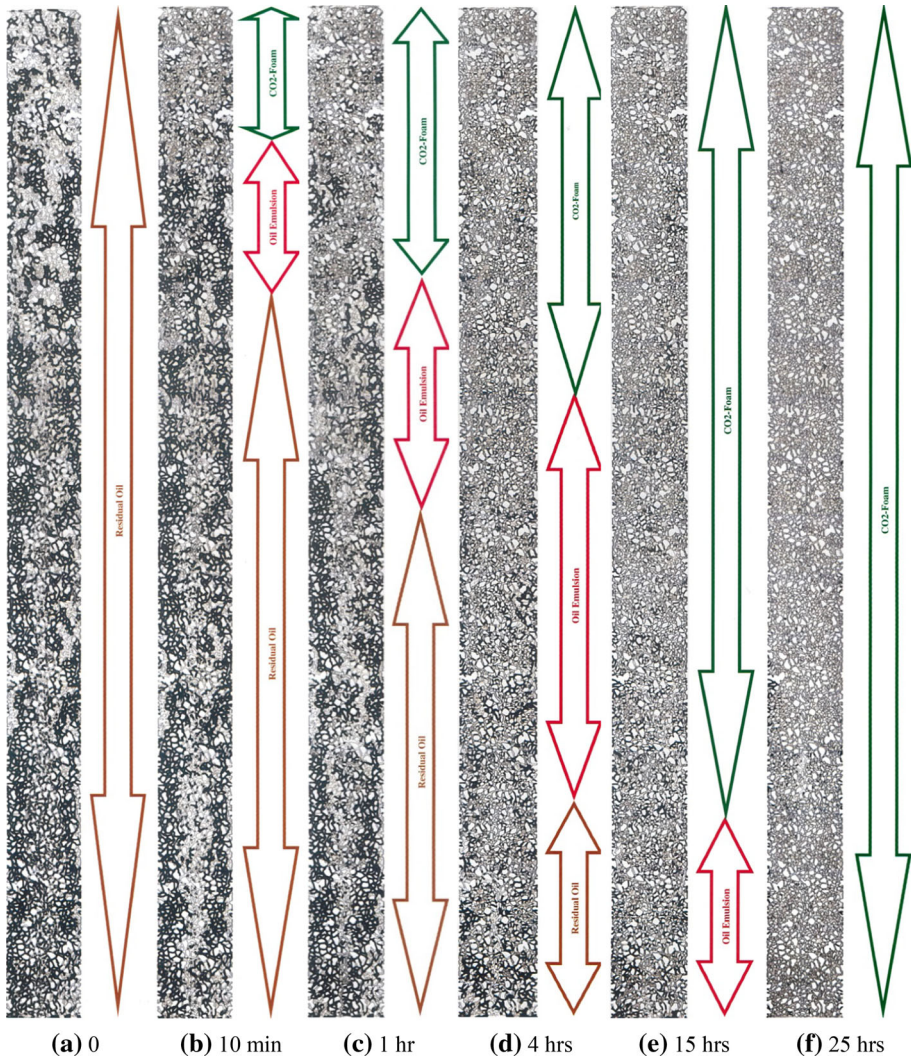


Fig. 23 Fluid distribution in the micromodel after **a** residual to AS flood, **b** 10 min, **c** 60 min, **d** 4 h, **e** 15 h and **f** 25 h of AS–CO₂-foam injection

experiments. There is no direct reaction between CO₂ and borate other than what is pH driven. Borate, a mild alkaline with natural pH of 10–11.9 and addition of carbonic acid (solution of CO₂ in water), will bring the pH down, converting it into other borates, such as borax (natural pH about 9.2–9.3). This produces a buffered system containing sodium carbonate, sodium bicarbonate, borax, etc., with compositions governed by the borate concentration and CO₂ partial pressure. Based on our results at the conditions of pressure and temperature, a mixture of AS solution and CO₂ did not react with each other in keeping the pH high enough or formation of oil in water emulsification. The favourable effects of borate appear to make the oil more non-spreading and therefore increase the strength and stability of foam in porous media.

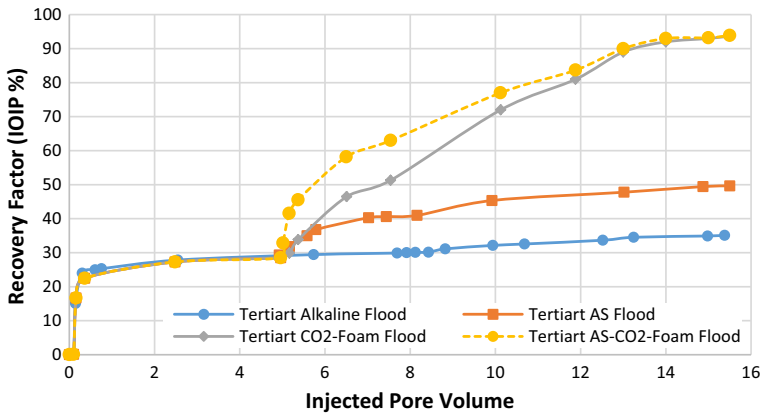


Fig. 24 Cumulative oil recovery versus injected fluids pore volume at different stages of the tertiary alkaline flood (Experiment 1), tertiary alkaline–surfactant flood (Experiment 2), tertiary CO₂-Foam flood (Experiment 3) and tertiary AS–CO₂-Foam flood (Experiment 4)

4 Quantitative Evaluations

Quantitative experimental results revealed that tertiary AS flood had comparable and higher macroscopic areal sweep efficiency as well as better oil recovery compared with tertiary alkaline flood (Fig. 24). The formation of O/W emulsion and changing wettability towards more water-wet conditions were responsible for higher oil recovery in case of AS flood. The interfacial tension reduction was not considered high enough using borate to produce emulsification of the oil in tertiary borate flood. Meanwhile, the initial wettability condition of this experiment was water wet; the change of wettability to more water wet due to injection of borate did not result in additional oil recovery during the borate injection period at tertiary mode. Figure 24 also reveals that the tertiary AS–CO₂-Foam flood had higher macroscopic sweep efficiency as well as better oil recovery in compared with tertiary AS flood. As CO₂ and the AS solutions entered the porous medium, the following events were observed: firstly, some the residual oil was displaced by the flowing CO₂. Secondly, due to the synergy effect of borate and the injected surfactant, an O/W emulsion phase was produced. Although borate and the surfactant are the main cause of the observed emulsion, the additional mixing caused by the flow of CO₂ facilitated the formation of the emulsion. Since the viscosity of O/W emulsions is much less than the heavy oil viscosity, the formation of these O/W emulsions helps significantly in increasing heavy oil recovery.

5 Conclusions

While CO₂-foam can increase oil recovery by some micro- and macro-scale mechanisms, addition of borate to surfactant can improve the performance of foam by producing more stable and stronger foams. As CO₂ and the AS solutions entered the porous medium, the following events were observed: firstly, some of the residual oil was displaced by the flowing CO₂. Secondly, due to the synergy of borate and C1 (surfactant), an O/W (oil in water) emulsion phase was produced. Although borate and the surfactant together are the main cause of the observed emulsion, the additional mixing caused by the flow of CO₂ facilitates

the formation of the emulsion. Since the viscosity of O/W emulsions is less than that of the oil, formation of the emulsion helps increase oil recovery. The results of this series of visual experiments reveal the successful application of borate for improving CO₂-foam characteristics and performance. The results will be used to design and perform similar core flood tests to quantify the performance of these processes and the impact on oil recovery and at the same time further investigate potential positive effects of CO₂-foam and borate.

Acknowledgements This work was performed as part of the Enhanced Heavy Oil Recovery joint industry project (JIP) in the Centre for Enhanced Oil Recovery and CO₂ Solutions of Heriot-Watt University. The JIP is equally funded by Total, ConocoPhillips, Eni, Pemex, and Wintershall, which is gratefully acknowledged.

Open Access This article is distributed under the terms of the Creative Commons Attribution 4.0 International License (<http://creativecommons.org/licenses/by/4.0/>), which permits unrestricted use, distribution, and reproduction in any medium, provided you give appropriate credit to the original author(s) and the source, provide a link to the Creative Commons license, and indicate if changes were made.

References

- Butler, R.M., McNab, G.S.: Theoretical studies on the gravity drainage of heavy oil during in situ steam heating. *J. Can. Petrol. Technol.* **59**, 455–460 (1981)
- Butler, R.M., Stephens, D.J.: The gravity drainage of steam heated heavy oil to parallel horizontal wells. *J. Can. Petrol. Technol.* **20**(2), 90–96 (1981)
- Dunning, H.N., Moore, J.W., Denekas, M.O.: Interfacial activities and porphyrin contents of petroleum extracts. *Ind. Eng. Chem.* **45**, 1759–1765 (1953)
- Emadi, A.: Enhanced Heavy Oil Recovery by Water and Carbon Dioxide Flood. Heriot-Watt University, Edinburgh (2012)
- Enick, R.M., Beckman, E.J., et al.: Direct thickeners for carbondioxide. In: SPE/DOE Improved Oil Recovery Symposium (2000)
- Farouq Ali, S.M.: Practical Heavy Oil Recovery 3–7(1997)
- Farzaneh, S.A., Dehghan, A.A., et al.: A comparative study of WAS, SWAS and solvent-soak scenarios applied to heavy oil reservoirs using 5-spot glass micromodels. *J. Can. Petrol. Technol.* **51**(5), 383–392 (2012)
- Farzaneh, S.A., Kharrat, R., et al.: Experimental study of solvent flooding to heavy oil in fractured five-spot micro-models: the role of fracture geometrical characteristics. *J. Can. Petrol. Technol.* **49**(3), 36–43 (2010)
- Farzaneh, S.A., Sohrabi, M.: A review of the status of foam application in enhanced oil recovery. In: 75th EAGE Conference & Exhibition incorporating SPE EUROPEC (2013)
- Farzaneh, S.A., Sohrabi, M.: Experimental investigation of CO₂-foam stability improvement by alkaline in the presence of crude oil. *Chem. Eng. Res. Des.* **94**, 375–389 (2015). <https://doi.org/10.1016/j.cherd.2014.08.011>. (ISSN 0263-8762)
- Farzaneh, S.A., Seyyedsar, S.M., Sohrabi, M.: Enhanced heavy oil recovery by liquid CO₂ injection under different injection strategies. *Soc. Petrol. Eng.* (2016). <https://doi.org/10.2118/181635-MS>
- Green, D.W., Willhite, G.P.: Enhanced Oil Recovery. Society of Petroleum Engineers, Dallas (1998)
- Guo, H., Faber, M.J., Buijse, M.A., Zitha, P.L.J.: A novel alkaline–surfactant-foam EOR process. *Soc. Petrol. Eng.* (2011). <https://doi.org/10.2118/145043-MS>
- Hirasaki, G.J., Lawson, J.B.: Mechanisms of foam flow in porous media: apparent viscosity in smooth capillaries. *SPEJ* **25**(2), 176–190 (1985)
- Huc, A.Y.: Heavy Crude Oils: From Geology to Upgrading An Overview. Editions Technip, Paris (2011)
- Klins, M.A.: Carbon dioxide Flooding: Basic Mechanisms and Project Design. International Human Resources Development Corporation, Boston (1984)
- Kovscek, A.R., Radke, C.J.: Fundamentals of Foam Transport in Porous Media in Foams: Fundamentals and Applications in the Petroleum Industry, ACS Advances in Chemistry Series, N. 242. American Chemical Society, Washington DC (1994)
- Kulkarni, M.M.: Immiscible and Miscible Gas–Oil Displacements in Porous Media. Louisiana State University, Craft and Hawkins Department of Petroleum Engineering, Baton Rouge (2003)
- Li, R.F., Yan, W., Liu, S.H., Hirasaki, G.J., Miller, C.A.: Foam mobility control for surfactant EOR. *SPEJ* **15**(4), 928–942 (2008)

- Lieu, V.T., Miller, S.G., Staphanos, S.J.: Long-term consumption of caustic and silicate solutions by petroleum reservoir sands. *Soluble Silicates Am. Chem. Soc. Symp. Ser.* **194**, 215–226 (1982)
- Martin, F.D., Oxley, J.C., Lim, H.: Enhanced recovery of a J sand crude oil with a combination of surfactant and alkaline chemicals. In: *SPE Annual Technical Conference and Exhibition* (1985)
- McKean, T.A.M., Thomas, A.H., et al.: Schrader bluff CO₂ EOR evaluation. In: *SPE Western Regional Meeting* (1999)
- Moritis, G.: Impact of production and development RD and D ranked. *Oil Gas J.* **93**(44), 34–36 (1995)
- Nasr-El-Din, H.A., Taylor, K.C.: Dynamic interfacial tension of crude oil/alkali/surfactant systems. *Coll. Surf.* **66**, 23–37 (1992)
- Nelson, R.C., Lawson, J.B., et al.: Co-surfactant-enhanced alkaline flooding. In: *The SPE/DOE Fourth Symposium on Enhanced Oil Recovery* (1984)
- Nguyen, Q.P., Currie, P.K., Buijse, M., Zitha, P.L.: Mapping of foam mobility in porous media. *SPEJ* **58**, 119–132 (2007)
- Pasquarelli, C.H., Wasan, D.T.: The effect of film-forming materials on the dynamic interfacial properties of crude oil–aqueous system. In: *The 3rd International Conference on Surface and Colloid Science* (1979)
- Pope, G.A., Nelson, R.C.: A chemical flooding compositional simulator. *SPEJ* **18**(5), 339–354 (1978)
- Reed, R.L., Healy, R.N.: Some physicochemical aspects of micro emulsion flooding: a review. In: *Improved Oil Recovery by Surfactant and Polymer Flooding*, pp. 382–437 (1977)
- Reisberg, J., Doscher, T.M.: Interfacial phenomena in crude oil–water systems. *Prod. Mon.* **21**, 43–50 (1956)
- Rossen, W.R.: Foams in enhanced oil recovery, chapter 12 in foams: theory, measurements and applications. In: Prud 'homme, R.K., Khan, S. (eds.) *Marcel Dekker, New York* (1996)
- Schramm, L.L.: Foam sensitivity to crude oil in porous media. Foams: fundamentals and applications in the petroleum industry. *Am. Chem. Soc.* **242**, 165–197 (1994)
- Seifert, W.K.: Carboxylic acids in petroleum sediments. In: *Progress in Chemistry of Natural Products*, Springer (1975)
- Shan, D., Rossen, W.R.: Optimal injection strategies for foam IOR. *SPEJ* **9**(2), 132–150 (2004)
- Shuler, P.J., Kuehne, D.L., Lerner, R.M.: Improving chemical flood efficiency with micellar/alkaline/polymer process. *JPT* (January) **41**, 80–88 (1989)
- Sohrabi, M., Henderson, G.D., Tehrani, D.H., Danesh, A.: Visualisation of oil recovery by water alternating gas (WAG) injection using high pressure micromodels-water-wet system. *Soc. Petrol. Eng.* (2000). <https://doi.org/10.2118/63000-MS>
- Sohrabi, M., Tehrani, D.H., Danesh, A., Henderson, G.D.: Visualization of oil recovery by water-alternating-gas injection using high-pressure micromodels. *Soc. Petrol. Eng.* (2004). <https://doi.org/10.2118/89000-PA>
- Sohrabi, M., Tehrani, D.H., Danesh, A., Henderson, G.D.: Visualisation of oil recovery by water alternating gas (WAG) injection using high pressure micromodels-oil-wet & mixed-wet systems. *Soc. Petrol. Eng.* (2001). <https://doi.org/10.2118/71494-MS>
- Upreti, S.R., Lohi, A., et al.: Vapor extraction of heavy oil and bitumen: a review. *Energy Fuels* **21**(3), 1562–1574 (2007)
- Zitha, P.L.J., Du, D.X.: A new stochastic bubble population model for foam flow in porous media. *Transp. Porous Media* **83**, 603–621 (2009)
- Zitha, P.L.J., Nguyen, Q.P., Currie, P.K., Buijse, M.A.: Coupling of foam drainage and viscous fingering in porous media revealed by X-ray computed tomography. *Transp. Porous Media* **64**(3), 301–313 (2006)